phys. stat. sol. (a) **205**, No. 8, 2052–2056 (2008) / **DOI** 10.1002/pssa.200778868

physica status solidi a
www.pss-a.com
applications and materials science

Optical properties of bismuth oxide thin films prepared by reactive d.c. magnetron sputtering onto p-GaSe (Cu)

Liviu Leontie[*, 1], **M. Caraman**[**, 2], **Igor Evtodiev**[3], **Elmira Cuculescu**[3], **and Ana Mija**[3]

[1] Faculty of Physics, "Al. I. Cuza" University, 11 Carol I Boulevard, 700506 Iasi, Romania
[2] University of Bacau, 157 Calea Marasesti, 600115 Bacau, Romania
[3] Moldova State University, 60 A Mateevici Str., 2009 Chisinau, Moldova

Received 12 June 2007, revised 29 March 2008, accepted 31 March 2008

PACS 61.10.Nz, 68.55.–a, 73.50.Pz, 78.20.Ci, 78.66.Li, 81.15.Cd

---

[*] Corresponding author: e-mail lleontie@uaic.ro, Phone: 0040-232-201168, Fax: 0040-232-201150
[**] e-mail mihailcaraman@yahoo.com

Bismuth oxide (Bi_2O_3) thin films with thickness in the range 20–160 nm have been deposited by d.c. reactive magnetron sputtering of Bi in an atmosphere $Ar:O_2$ (1 : 1), onto single crystalline p-GaSe (Cu) substrates. The optical constants, *n* and *k*, of oxide films have been determined from the analysis of the polarization ellipse of the reflected radiation from outer surface of Bi_2O_3/p-GaSe structures. In the wavelength range 400–800 nm the refractive index of nanometric Bi_2O_3 films onto GaSe(Cu) decreases from 2.10 to 1.78 and it seen to increase at decreasing sample thickness. In order to determine the interaction mechanism between semiconducting oxide film and GaSe surface, the spectral characteristics of photocurrent through Bi_2O_3/p-GaSe junction and optical absorption in the range 400–800 nm have been examined. As resulted from respective analyses, Bi_2O_3 film generates new valence bonds, which contribute to the increase in the density of localized states at Bi_2O_3/p-GaSe (Cu) junction interface.

1 Introduction Bismuth oxide (Bi_2O_3) is a representative semiconducting oxide material, showing optical transparency over a wide wavelength range and significant values of bandgap, refractive index and dielectric permittivity, as well as marked photoconductivity and photoluminescence [1–3]. Owing to their peculiar characteristics, its thin-film polymorphs are widely used in modern solid-state technology, in particular, as optical coatings for optoelectronic devices [4, 5].

As was shown in a series of previous papers [1–3], the optical and electrical properties of bismuth oxide thin films are strongly dependent on both characteristics of deposition method, which moulds the phase composition of samples, and substrate nature.

III–VI semiconductors crystallize in form of chalcogen–metal–metal–chalcogen (for gallium selenide, Se–Ga–Ga–Se) stratified packages. The chemical bonds between four monoatomic sheets inside a package have ionic-covalent nature, while between packages are of Van der Waals type [6]. GaSe single crystal shows a selenium-terminated surface, with closed valence bonds. Presence of a different nature layer leads to formation of new valence bonds at GaSe surface and consequently, can exert a substantial influence on electron energy spectrum for both oxide layer and substrate. In particular, a semiconducting oxide coating onto semiconductor substrate is able to modify the energy spectrum of surface states in the substrate material, allowing selective adsorption of gaseous molecules from the ambient [7].

The characteristics of optoelectronic devices based on semiconductor–oxide structures are determined by optical properties of components and charge carrier transport mechanism through interface layer [8].

This work focuses on the investigation of optical properties of bismuth oxide films sputtered onto (0001) surface of Cu-doped GaSe single crystals and amorphous SiO_2. Besides, from experimental study of optical absorption in single-crystalline GaSe(Cu) layers and of photosensitivity for Bi_2O_3/GaSe(Cu) structures, the influence of semiconducting oxide film on GaSe surface is examined.

2 Experimental

GaSe single crystals have been grown by Bridgmann method [9]. Cu doping with a concentration 6.8×10^{17} cm^{-3} has been achieved during chemical synthesis of GaSe.

In experiments ε-GaSe single-crystalline samples with p-type conductivity have been used. Besides, for comparison, specially undoped GaSe single crystals have been examined, for which $N_A - N_D = 10^{12}$ cm^{-3}, where N_A and N_D are acceptor and donor concentrations, respectively.

Bismuth oxide thin films were deposited by rf (40.68 MHz) reactive magnetron sputtering onto amorphous quartz and single-crystalline GaSe(Cu) layers at room temperature ($T = 293$ K), at a chamber pressure of 10^{-3} Torr, in an atmosphere Ar:O_2 (2:1). Bi (99.999%) metal was used as sputtering target material.

The crystalline structure of bismuth oxide films and Bi_2O_3/GaSe(Cu) structures was examined by X-ray diffraction (XRD), using a DRON-2 apparatus (Cu K_α radiation, $\lambda = 1.5418$ Å).

In the study of the transmission and reflection spectra of bismuth oxide films and single-crystalline GaSe(Cu) layers a double-beam SPECORD UV–VIS M-40 spectrophotometer was used.

In the region of fundamental absorption edge, the absorption coefficient (α) of plan-parallel sample with thickness d was determined by using the relationship [10]:

$$T = [(1-R)^2 \exp(-\alpha d)]/[1 - R^2 \exp(-2\alpha d)]\,, \tag{1}$$

valid for normal incidence and in absence of interference effects, where T and R denote the transmission and reflection factors, respectively.

The thickness of bismuth oxide films in the range $d \geq 100$ nm was measured by an interferometric method [11]. For thinner films both thickness and dispersion of optical functions n and k (the refractive index and the extinction coefficient, respectively) were determined from the analysis of the polarization ellipse for reflected radiation from the sample surface. The optical constants have been determined by using the following equations [12]:

$$n^2 - k^2 = \sin^2\varphi \left[1 + \mathrm{tg}^2\,\varphi\, \frac{\cos^2 2\rho - \sin^2 2\rho \sin^2 \Delta}{(1 - \sin^2 2\rho \cos \Delta)^2}\right] \tag{2}$$

and

$$nk = \sin^2\varphi\, \mathrm{tg}^2\,\varphi\, \frac{\sin 2\rho \cos 2\rho \sin \Delta}{(1 - \sin^2 2\rho \cos \Delta)^2}\,, \tag{3}$$

where φ is the angle of polarization (in the vicinity of the Brewster angle) of the incident light, Δ is the phase difference between waves with polarizations "p" and "s" (parallel and perpendicular to the incidence plane, respectively), and $\rho = \mathrm{arctg}\sqrt{R_p/R_s}$ (with R_p and R_s denoting reflectances for two polarizations). The spectral characteristics $\Delta(\lambda)$ and $\rho(\lambda)$ in the range 400–800 nm have been recorded by a photometric equipment including a monochromator with diffraction grating (600 mm^{-1}). Glann–Thompson prisms were used to set linear light polarization and to analyze polarization state of the reflected radiation (together with a quartz compensator).

The photoelectromotive force generated by Bi_2O_3/GaSe(Cu) structure was measured by a V7–30 electrometer with an input resistance of $\sim 10^{14}$ Ω.

3 Results and discussion

XRD analyses (Fig. 1) indicate presence of three main phases in examined bismuth oxide/GaSe(Cu) structures. Together with two intense peaks of ε-GaSe located at 28° and 49°, assigned to crystalline planes (103) and (1014), respectively, two reflections characteristic to bismuth oxide can be evidenced and they belong to β-Bi_2O_3 and δ-Bi_2O_3. Their line profiles are rather wide, which indicates polycrystalline nature of the semiconducting oxide layer. Crystallite mean dimension (D) was estimated by means of Debye–Scherrer's formula [13]:

$$D = 0.94\lambda/a \cos\theta\,, \tag{4}$$

where λ is X-ray wavelength, θ is Bragg diffraction angle, and a is angular full width at half maximum intensity (FWHM). For 113 nm thick films, the resulted mean dimension of β-Bi_2O_3 crystallites is about 56 nm. As structure investigations show (Fig. 1), the phase composition of

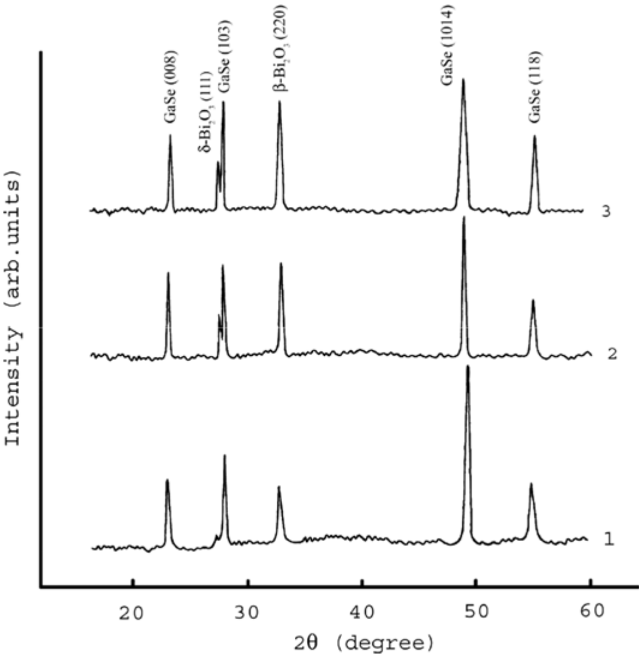

Figure 1 XRD patterns for Bi_2O_3/GaSe(Cu) structures; thickness of bismuth oxide film: 1 – $d = 28$ nm; 2 – $d = 113$ nm; 3 – $d = 157$ nm.

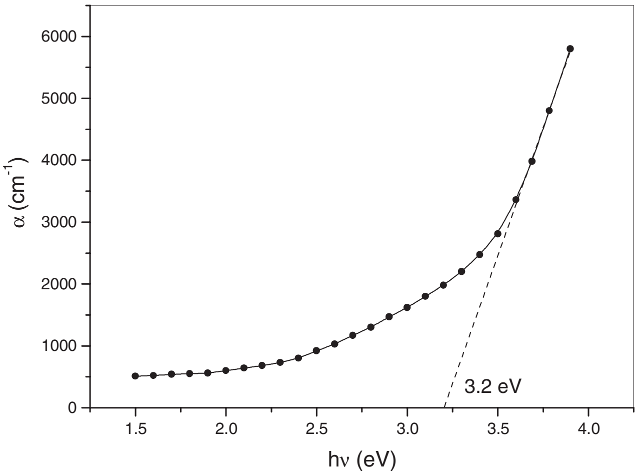

Figure 2 Spectral dependence of the absorption coefficient of Bi_2O_3 films onto SiO_2.

bismuth oxide films (β- and δ-Bi_2O_3) is not influenced by film thickness

The optical absorption of bismuth oxide samples was examined. In Fig. 2 the absorption spectrum of bismuth oxide films onto SiO_2 is illustrated. For samples with thickness between 26 nm and 153 nm the absorption coefficient, as determined from Eq. (1), ranged between 6×10^3 cm^{-1} and 480 cm^{-1}. By extrapolating the linear part of $\alpha(h\nu)$ curves to zero value of the ordinate the optical bandgap (E_{go}) of polycrystalline diphasic bismuth oxide films at room temperature (293 K) can be determined and was found as 3.2 eV.

One can observe that in the high transparency spectral region ($h\nu < E_{go}$), the obtained values of the absorption coefficient (α) also include radiation losses due to microstructural defects (intercrystallite boundaries, presence of crystalline phases with different optical constants, etc.). These losses are also responsible on variation of α with sample thickness. In order to suppress the influence of film thickness, the spectral characteristics of the extinction coefficient (k) and refractive index (n) have been calculated from the analysis of the polarization ellipse for reflected light at bismuth oxide-air interface, by means of Eqs. (2) and (3).

Figure 3a shows dispersion of the extinction coefficient $k(\lambda)$ for bismuth oxide films with different thickness ($d = 63$ nm and $d = 158$ nm), deposited onto (0001) surface of Cu-doped GaSe (0.05 at%). As can be observed from this figure, in the spectral range 400–800 nm the extinction coefficient is decreasing from 7×10^{-3} to 3.1×10^{-3}. At the same time, for a fixed wavelength, its value is seen to increase at decreasing sample thickness, indicating an additional absorption of thinner samples, which is due to increased role of surface absorption (transitions occuring on the surface energy states) in comparison to the bulk absorption. Curve 1 (Fig. 3a) illustrates dispersion of the extinction coefficient calculated from α values (Fig. 2). As can be ascertain from comparison of curves 1–3, the optical functions of substrate (especially its refractive index) exert a sensible influence on the value of the extinction coefficient of bismuth oxide films.

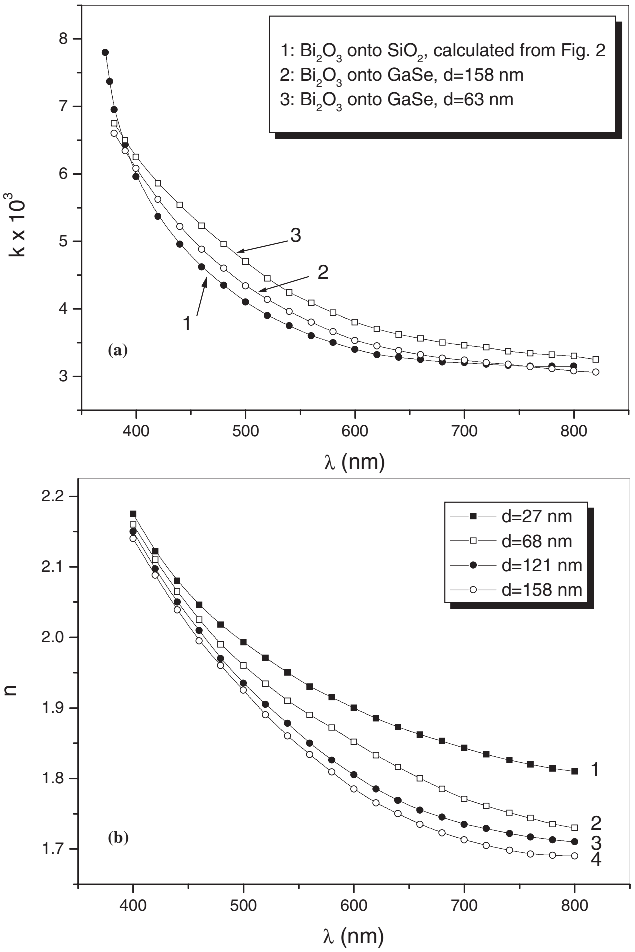

Figure 3 Spectral dependence of the extinction coefficient for Bi_2O_3 films: (a) 1 – onto SiO_2, calculated from spectral characteristics in Fig. 2; 2 – onto GaSe, thickness $d = 158$ nm; 3 – onto GaSe, $d = 63$ nm. (b) Dispersion of refractive index of Bi_2O_3 films onto GaSe(Cu).

The slow decrease of the extinction coefficient in a rather wide photon energy range, 3.8–1.5 eV, indicates presence of a substantial spectrum of energy states within semiconductor bandgap. This is strongly influenced by lattice deformations and electric fields that manifest at grain boundaries within polycrystalline thin-film samples. Their influences are very likely, taking into account polycrystalline and diphasic (β- and δ-Bi_2O_3) nature of actual oxide films.

A similar spectral dependence can be observed for the dispersion of the refractive index $n(\lambda)$ (Fig. 3b). The refractive index of bismuth oxide film with thickness 158 nm is seen to decrease from 2.18 to 1.69, for wavelengths in the range 400–800 nm. Besides, for a fixed wavelenght, it is increasing at decreasing sample thickness, in the case of bismuth oxide films onto GaSe(Cu). We mention that

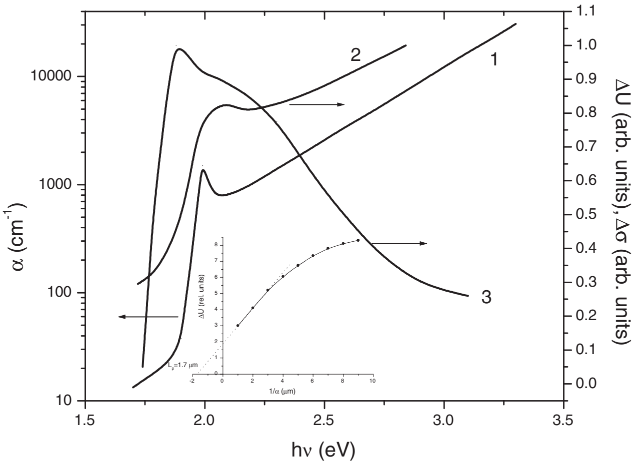

Figure 4 1 – Spectral characteristics of the absorption coefficient of single-crystalline GaSe(Cu) layers; 2 – Spectral characteristics of the photoconductivity for GaSe(Cu) layers; 3 – Spectral distribution of the open-circuit voltage for Bi_2O_3/GaSe(Cu) structure. Thicknesses: Bi_2O_3 films – 130 nm; GaSe(Cu) layer – 12 μm. Doping content: 0.05 at% Cu. Inset: Plots of the open-circuit voltage vs. inverse of absorption coefficient for the Bi_2O_3/GaSe(Cu) junction.

this behavior is more pronounced for smaller thickness samples.

Figure 4 presents the absorption spectrum of single-crystalline GaSe(Cu) layers (curve 1), their photoconductivity spectral characteristics (curve 2), as well as the spectral dependence of the open-circuit voltage (ΔU) for Bi_2O_3/GaSe(Cu) junction illuminated through Bi_2O_3 layer (curve 3).

As can be observed from curves 1 and 2, at photon energies $h\nu > 2.1$ eV the photoconductivity of single-crystalline GaSe(Cu) layers increases together with the absorption coefficient α. If one takes into account that actual thickness of GaSe layer (about 12 μm) fulfills the condition for complete photon absorption within sample, $\alpha d \gg 1$, then one can consider that photoconductivity is proportional to total number of absorbed photons, A:

$$\Delta\sigma \sim A \cdot \tau\,, \tag{5}$$

where τ is lifetime of nonequilibrium charge carriers. For a low-level excitation of sample, it can be considered to be constant.

The linear increase of the absorption coefficient and photoconductivity in the depth of the fundamental absorption band do attest small recombination rates of the non-equilibrium charge carriers through surface states in GaSe(Cu) layers.

When exciting Bi_2O_3/GaSe(Cu) structure (by illuminating through Bi_2O_3 film) with photons of energy $h\nu > 1.7$ eV, separation of non-equilibrium charge carriers within junction occurs. The open-circuit voltage (ΔU) reaches its maximum for the energy corresponding to Cu impurity absorption band ($h\nu \approx 1.88$ eV) and tends to markedly decrease at increasing photon energies. Taking into account that the edge of the absorption band of GaSe(Cu) layer actually coincides with that of $\Delta U(h\nu)$ spectral characteristics, as well as the magnitude of α, one can consider that generation of non-equilibrium charge carriers takes place in an about 1–10 μm thick GaSe(Cu) layer by Bi_2O_3/GaSe(Cu) interface. The slow decrease of ΔU at increasing α values indicates presence of short lifetime surface states; these are produced by atoms inside Bi_2O_3 layer, which form new valence bonds with Se atoms by surface of Se–Ga–Ga–Se package.

If one consider that $\alpha d_n \ll 1$, where the depth of generation of non-equilibrium charge carriers in GaSe(Cu) layer by junction interface (d_n) is lesser than hole diffusion length (L_p), and recombination rate at Bi_2O_3/GaSe(Cu) interface is independent on the exciting level (illumination intensity), then the open-circuit voltage can be described by a monotonic function of $\alpha J_0/(\alpha L_p + 1)$ [14], where J_0 is the flux of the incident photons. By analyzing $\Delta U(1/\alpha)$ dependence (Fig. 4 Inset) hole diffusion length in GaSe(Cu) layer by Bi_2O_3/GaSe(Cu) interface can be determined. By extrapolating the linear part of this curve to the abscissa axis, $L_p \approx 1.7$ μm was found.

4 Conclusion

RF reactive magnetron sputtering of Bi targets onto GaSe(Cu) in an atmosphere Ar:O_2 (2:1) leads to deposition of polycrystalline diphasic (β- and δ-Bi_2O_3) bismuth oxide films.

The optical bandgap of bismuth oxide films onto amorphous quartz at temperature $T = 293$ K is equal to 3.2 eV.

As resulted from the analysis of the polarization ellipse for the reflected light from Bi_2O_3/GaSe(Cu) junction, in the spectral range 400–800 nm both optical functions $n(\lambda)$ and $k(\lambda)$ of bismuth oxide films onto single-crystalline GaSe(Cu) decrease with increasing film thickness.

Bi_2O_3/GaSe(Cu) junctions show photogeneration properties for photon energy range 1.5–3.0 eV.

Presence of Bi_2O_3 film leads to formation of new valence bonds at GaSe(Cu) crystal surface, resulting in increasing density of short lifetime surface states.

By analyzing spectral characteristics $\alpha(h\nu)$ and $\Delta U(h\nu)$ hole diffusion length in the Bi_2O_3/GaSe(Cu) junction layer was found as 1.7 μm.

Acknowledgements This work was supported by National Authority for Scientific Research (ANCS), Minister of Education and Research, Romania, through CEEX grants no. 2/01.08.2006 (code 06-11-51-1) and FOTONTECH. Authors would like to greatly thank Professor G.I. Rusu for many fruitful discussions.

References

[1] L. Leontie, M. Caraman, and G. I. Rusu, J. Optoelectron. Adv. Mater. **2**, 385 (2000).

[2] L. Leontie, M. Caraman, A. Visinoiu, and G. I. Rusu, Thin Solid Films **473**, 230 (2005).

[3] L. Leontie, J. Optoelectron. Adv. Mater. **8**, 1221 (2006).

[4] V. Fruth, M. Popa, D. Berger, R. Ramer, M. Gartner, A. Ciulei, and M. Zaharescu, J. Eur. Ceram. Soc. **25**, 2171 (2005).

[5] G. Bandoli, D. Barecca, E. Brescacin, G. A. Rizzi, and E. Tondello, Chem. Vapor Depos. **2**, 238 (1996).

[6] E. Cuculescu, Ig. Evtodiev, M. Caraman, and L. Leontie, J. Optoelectron. Adv. Mater. **8**, 112 (2006).

[7] G. Korotcencov, Sens. Actuators B **107**, 209 (2005).

[8] H. Hosono, Thin Solid Films **515**, 6000 (2007).

[9] Ph. Schmid, J. P. Voitchovsky, and A. Mercier, phys. stat. sol. (a) **21**, 443 (1974).

[10] Yu. I. Uchanov, Optičeskie Svoistva Poluprovodnikov (Nauka, Moskva, 1977), p. 75.

[11] R. W. Ditchburn, Light (Blackie & Son Ltd., London, Glasgow, 1965).

[12] H. R. Phillip and H. Ehrenreich, Semicond. Semimet. **3**, 93 (1967).

[13] B. E. Warren, X-ray Diffraction (Dover, New York, 1990), p. 253.

[14] Y. Marfaing, in: Handbook on Semiconductors, Optical Properties of Semiconductors, edited by T. S. Moss and M. Balkanski (North-Holland, Elsevier, Amsterdam, 1994), p. 758.